Metallomics

Accepted Manuscript

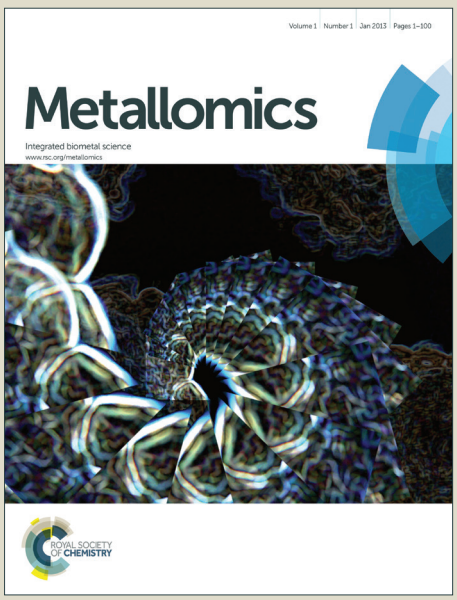

ROYAL SOCIETY OF CHEMISTRY

www.rsc.org/metallomics

Quantitative bioimaging by LA–ICP-MS: a methodological study on the distribution of Pt and Ru in viscera originating from cisplatin- and KP1339-treated mice

Alexander E. Egger*[1,2], Sarah Theiner[2,3], Christoph Kornauth[4], Petra Heffeter[3,5], Walter Berger[3,5], Bernhard K. Keppler[2,3], Christian G. Hartinger*[2,3,6]

[1] ADSI – Austrian Drug Screening Institute GmbH, Innsbruck, Austria

[2] Institute of Inorganic Chemistry, University of Vienna, Vienna, Austria

[3] Research Platform 'Translational Cancer Therapy Research', University of Vienna, Vienna, Austria

[4] Institute of Clinical Pathology, Medical University of Vienna, Vienna, Austria

[5] Institute of Cancer Research, Department of Medicine I, and Comprehensive Cancer Center, Medical University of Vienna, Vienna, Austria

[6] School of Chemical Sciences, University of Auckland, Auckland, New Zealand

* Corresponding Authors: ADSI, Innrain 66a, A-6020 Innsbruck, Austria, E-Mail: alexander.egger@adsi.ac.at, Tel.: +43-512-507-36305 (A.E.E); University of Auckland, School of Chemical Sciences, Private Bag 92019, Auckland 1142, New Zealand E-mail: c.hartinger@auckland.ac.nz, Fax: (+64)9 373 7599 ext 87422 (C.G.H.)

ABSTRACT

Laser ablation-inductively coupled plasma-mass spectrometry (LA–ICP-MS) was used to study the spatially-resolved distribution of ruthenium and platinum in viscera (liver, kidney, spleen, and muscle) originating from mice treated with the investigational ruthenium-based antitumor compound KP1339 or cisplatin, a potent, but nephrotoxic clinically approved platinum-based anticancer drug. Method development was based on homogenized Ru- and Pt-containing samples (22.0 and 0.257 µg/g, respectively). Averaging yielded satisfactory precision and accuracy for both concentrations (3–15% and 93–120%, respectively), however when considering only single data points, the highly concentrated Ru sample maintained satisfactory precision and accuracy, while the low concentrated Pt sample yielded low recoveries and precision, which could not be improved by use of internal standards (^{115}In, ^{185}Re or ^{13}C). Matrix-matched standards were used for quantification in LA–ICP-MS which yielded comparable metal distributions, *i.e.*, enrichment in the cortex of the kidney in comparison with the medulla, a homogenous distribution in the liver and the muscle and areas of enrichment in the spleen. Elemental distributions were assigned to histological structures exceeding 100 µm in size. The accuracy of a quantitative LA–ICP-MS imaging experiment was validated by an independent method using microwave-assisted digestion (MW) followed by direct infusion ICP-MS analysis.

GRAPHICAL ABSTRACT

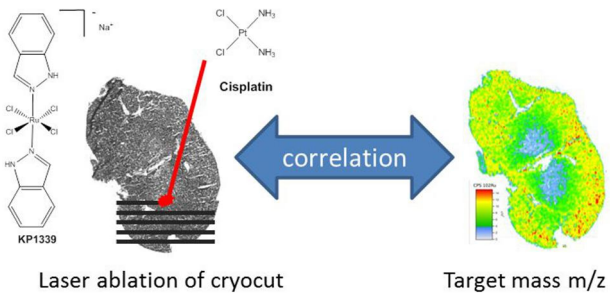

In a methodological study, quantitative LA–ICP-MSI was used to compare the distribution of Pt and Ru in viscera from cisplatin- and KP1339-treated mice

INTRODUCTION

Metal-based drugs possess a long and successful history in anticancer treatment, starting in 1978 with the worldwide approval of cisplatin (Figure 1).[1,2] Despite being highly efficient in treatment of testicular, head, neck and ovarian tumours, patients suffer from severe side effects such as emesis, neurotoxicity and myelosuppression as well as nephrotoxicity, which is often dose-limiting.[3,4] Nevertheless, cisplatin and its second and third generation compounds carboplatin and oxaliplatin are still among the most frequently prescribed anticancer agents nowadays.[5,6] Promising alternatives to platinum-based therapeutics aim for reduced side effects and efficacy in resistant tumours. These include ruthenium-based anticancer complexes, for example sodium *trans*-[tetrachloridobis(1*H*-indazole)ruthenate(III)], KP1339 (Figure 1), which is currently undergoing a clinical phase I/II trial.[7-11]

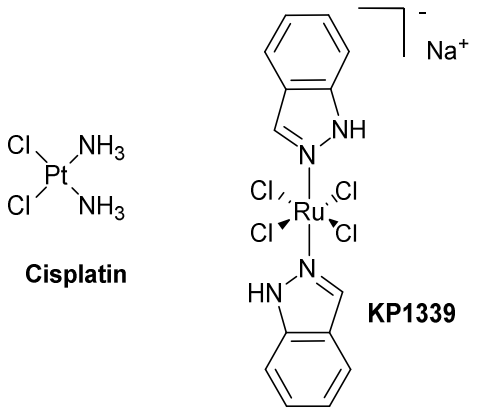

Figure 1: Chemical structures of the clinically established anticancer compound cisplatin as well as the investigational ruthenium complex KP1339.

Despite intensive preclinical testing, the main reasons causing abandonment of clinical trials include issues with the pharmacokinetics of drug candidates, low efficacy and unexpected side effects.[12,13] Bioimaging techniques in preclinical *in vivo* studies could improve the success rate by visualizing the distribution of a drug in the target tissue with high spatial resolution in the micrometre scale at an early stage in the drug development process. Highly sensitive imaging techniques based on mass spectrometry such as laser ablation-inductively coupled plasma-mass spectrometry (LA–ICP-MS), matrix-assisted laser desorption ionization-mass spectrometry (MALDI-MS), and secondary ion mass spectrometry (SIMS) serve as analytical tools in biomedical studies as well as in the fields of medicinal and bioinorganic chemistry.[14-18] LA–ICP-MS has become the method of choice in elemental bioimaging as it combines the high spatial resolution of laser ablation (spot size down to 4 µm) with the high sensitivity of mass spectrometric detection by ICP-MS yielding detection limits in the sub µg/g range, especially for transition metals.[17,19] Furthermore, the sample preparation is

straightforward, as the tissue samples are either paraffin-embedded or cryocut onto glass slides, with the tissue thickness varying in the range from 5 to 200 μm.[18,20] A general work-flow for a bioimaging experiment is depicted in the supporting information (Scheme S1). Quantification is mainly hampered by the lack of appropriate certified reference materials for the analyte of interest in the respective tissue-based matrix and a standardized approach for the application of internal standards in the analyses has not been established.

One of the major challenges of LA–ICP-MS in bioimaging studies is the development of reliable and validated quantification strategies.[18,21] Several quantification procedures have been proposed in the literature including online-addition of solution-based calibration standards[19,22] and standards spiked in polymers followed by coating on slides.[23] Most commonly, matrix-matched calibration standards are individually prepared for each analytical problem by homogenization of the matrix (*e.g.*, whole blood/blood serum, chicken breast, liver and rat brain tissues) and addition of a defined amount of the analytes of interest.[19,24-26] As the analysis time per sample is typically in the range of several hours, the development of strategies to account for variations of the elemental response are challenging. They are caused by, *e.g.*, varying water content in the sample and different sample thickness, fluctuations in the laser chamber during the ablation process and during quantification by ICP-MS. To account for these issues, a suitable internal standard needs to be used, which ideally is a naturally occurring and homogenously distributed element within the biological matrix. Consequently, the isotope ^{13}C has been shown to be the element of choice for tissue samples. The main drawbacks of ^{13}C are the significantly different atomic mass and first ionization potential compared to most analytes as well as its insensitivity to instrumental fluctuations of the ICP-MS.[27,28] Iodine as an internal standard has been proposed upon iodination of cell nuclei in fibroblast cells and has allowed correction for tissue inhomogeneities.[29,30] Further strategies involve spin-coating of the glass slide with solutions of the internal standard and placing the sample tissue on top.[23] Alternatively, a thin layer of a gold standard can be deposited directly on the tissue.[31] Both strategies yield simultaneous ablation of the sample and the internal standard.

In biomedical studies, LA–ICP-MS has shown high potential to improve the understanding of the distribution of trace elements involved in complex biological processes at tissue and cellular level. Especially analysis of metal-based nanoparticles yielded spatially-resolved elemental distributions in the nanometre scale allowing assignment to subcellular structures.[29,32-34] Several studies have focussed on bioimaging of brain samples from animal models for Parkinson's, Alzheimer's and Wilkinson's disease and disease-induced alterations of elements were monitored.[19,22,35-38] In cancer research, LA–ICP-MS has been used to map the metabolism and pathogenesis of primary brain tumours,[39,40] to identify metastatic melanoma in lymph nodes,[41] and to detect tumor markers in breast cancer tissue.[20] In the field of platinum-based anticancer drugs, metal distribution in tissues

being targeted by cisplatin (testis, kidney and cochlea) has recently been determined by LA–ICP-MS.[42-44] Furthermore, ICP-MS and LA–ICP-MS have been combined to study the uptake of oxaliplatin by hyperthermic intraperitoneal chemotherapy in rats.[45]

Within this paper, we compared for the first time the (quantitative) spatially-resolved biodistribution of Ru and Pt in viscera (kidney, liver, muscle, and spleen) of KP1339- or cisplatin-treated Balb/c mice. Additionally, the validation of the method is reported. This includes analysis of homogenates of known metal concentrations by LA–ICP-MS as well as the application of microwave digestion followed by direct infusion ICP-MS measurements as an independent method for proving the validity of the data.

EXPERIMENTAL

Chemicals

Cisplatin and KP1339 were prepared according to literature procedures.[46,47] Nitric acid (≥65%, p.a.) was purchased from Fluka (Buchs, Switzerland) and further purified in a quartz sub-boiling point distillation unit (Milestone-MLS GmbH, Leutkirch, Germany). All dilutions were gravimetrically prepared with Milli-Q water (18.2 MΩ cm, Milli-Q Advantage, Darmstadt, Germany). Indium, platinum, rhenium, and ruthenium standards were obtained from CPI International (Amsterdam, The Netherlands). Tissue-Tek medium (Sakura Finetek, Netherlands) was used for the embedding of the cryocuts.

Animal experiments

Eight-week-old Balb/c mice were purchased from Harlan Laboratories (San Pietro al Natisone, Italy). The animals were kept in a pathogen-free environment and every procedure was done in a laminar airflow cabinet. Animal experiments were approved by the ethics committee of the Medical University of Vienna and the Bundesministerium für Wissenschaft und Forschung Ref. II/10b (Gentechnik und Tierversuche), application Nr. BMWF-66.009/0337-II/3b/1011, and were carried out according to the Austrian and FELASA guidelines for animal care and protection in order to minimize distress for the animals. Mice (n = 2 for each treatment) were treated with 15 mg/kg cisplatin intraperitoneally (in 0.9% NaCl) or 50 mg/kg KP1339 intravenously (in citrate buffer pH 3.5). Mice were sacrificed after 18 or 24 h for KP1339 and cisplatin, respectively. The entire liver of one mouse per group was removed and stored at -20°C for method development. Organs of the second mouse (liver, kidney, muscle and spleen) were used for the determination of the biodistribution of Pt and Ru, and its quantification by LA–ICP-MS and ICP-MS after MW digestion. Tissues for imaging were

either immediately frozen in dry ice-cooled methylbutane or stored at 4 °C if cryocutting could be performed within 5 h. Additional samples of all organs were stored at -20 °C for quantitative determination of the respective average metal concentration by means of MW and ICP-MS analysis. Half of a kidney from each animal group was formalin-fixed and paraffin-embedded for detailed histopathological evaluation *via* periodic acid Schiff (PAS) stain.

Preparation of standards and controls

Commercially available pig liver (approx. 5 g) was used for the preparation of matrix-matched standards, spiked with In and Re (10 µg/g each) and homogenized with a ball homogenizer (Schwingmuehle Retsch MM2000) with a single ceramic ball for 5 min at 40% and 5 min at 90% intensity. Aliquots were spiked with liquid Ru and Pt standards yielding final concentrations ranging from 1 to 50 µg/g. In order to minimize dilution of the matrix, the total amount of added standard solution never exceeded 10% (w/w). Mixing of homogenates with standard solutions was performed in Eppendorf tubes together with 3 balls made from steel at 70% energy for 15 min.

In order to check the accuracy of the method in general, control samples containing a known concentration of analyte were prepared independently of the standards in the following manner: liver (approx. 1 g) from cisplatin- or KP1339-treated mice, which was not subjected to bioimaging experiments and thus independent, was spiked with In and Re (10 µg/g each) and homogenized following the protocol for the preparation of the standards. Samples were pelletized in an Eppendorf centrifuge at 80 rpm for 1 min. Subsequently, the standards and control samples were prepared by microwave-assisted digestion for direct infusion ICP-MS to verify the concentration of the standards and to determine the target value (“true value”) for the LA-ICP-MS control samples (Scheme 1). The remaining homogenates were stored at -20 °C.

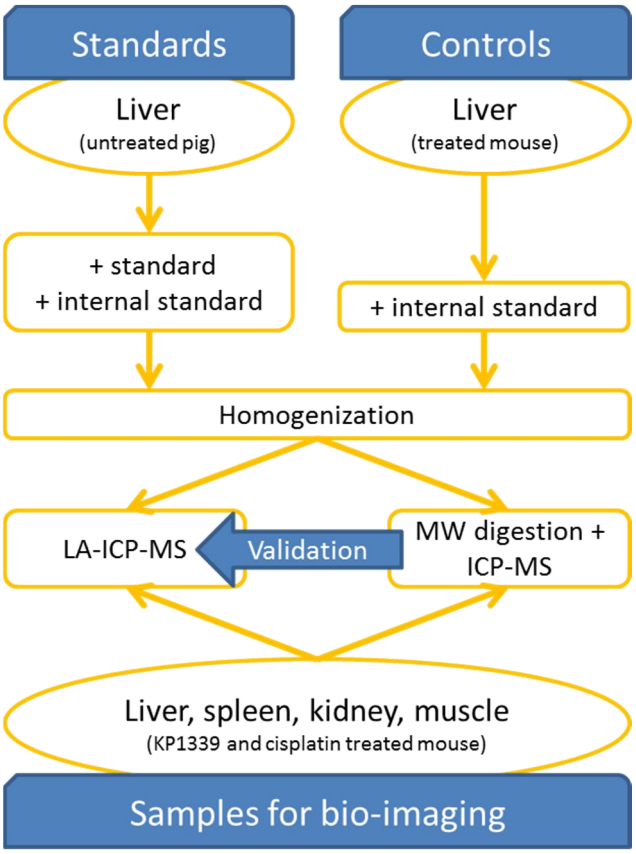

Scheme 1: Simplified overview of sample preparation. Standards (spiked with known amounts of Ru or Pt as well as internal standards) and control samples (originating from a treated animal) were homogenized and analyzed via LA–ICP-MS and MW digestion followed by ICP-MS measurement for method development and validation. The metal content in samples originating from animal experiments was quantified by these two methods in the same manner using MW digestion as reference for proving validity of the data obtained by LA–ICP-MS.

Quantification of the average metal content by ICP-MS

An ETHOS microwave digestion system (MLS, Leutkirch, Germany), equipped with an MR-10 rotor for 30 QS-3 teflon tubes was used. Prior to sample digestion, all tubes were cleaned with equal volumes of water and nitric acid of subboiled quality at 180 °C for 20 min under temperature control of one vessel. Consecutively, the samples with a moist mass of 20–40 mg (*i.e.*, tissues from animal experiments, standards, and controls; see Scheme 1) were digested with 35% nitric acid using the conditions given in Table S1 (see Supporting Information). Samples were diluted with Milli-Q water yielding a nitric acid concentration of approx. 3.5% and metal concentrations not exceeding 15 ng/g. An ICP-MS (Agilent 7500ce, Waldbronn, Germany) equipped with a CETAC ASX-520 autosampler (Nebraska, USA) and a MicroMist nebulizer at a sample uptake rate of approximately 0.25 ml/min was used for quantification. In and Re served as internal standards for Ru and Pt, respectively, in samples originating from animal experiments. As the homogenates (standards and control samples) already contained In and Re, Ce was used in that case alternatively. The internal standard was added *via* a peristaltic pump and merged with the solution of the analyte *via* a T-piece previous to the

nebulizer. Experimental parameters are summarized in Table 1. Data processing was conducted with the MassHunter software package (Agilent, Workstation Software, Version B.01.01, 2012). If not otherwise stated, reported data is based on digestions performed in triplicates. As a certified reference material for Ru and Pt in mammalian tissue is to the best of our knowledge not available, three to five samples, which were analyzed on different days with independently prepared calibration standards, were used as control samples for the current calibration to ensure lab-internal long term comparability of measured data.

Table 1: Parameters for the quantification of liquid samples by ICP-MS and for the hyphenation with a laser ablation system

	ICP-MS	**LA–ICP-MS**
RF-Power [W]	1500	1350
Cones	Ni	Ni
Registered Isotopes	^{101}Ru, ^{102}Ru, ^{115}In, ^{140}Ce, ^{194}Pt, ^{195}Pt, ^{185}Re	^{13}C*, ^{102}Ru, ^{115}In*, ^{185}Re*, ^{195}Pt
Dwell time [s]	0.1	0.1
Replicates	10	not meaningful
Carrier gas [l/min]	0.9	1.0
Make up gas [l/min]	0.2	-
Plasma gas [l/min]	15	15

* Internal standards were only registered in spiked, homogenized samples used for method development

Laser ablation and data processing

Sample preparation. Matrix-matched homogenous liver standards, homogenized liver originating from cisplatin- or KP1339- treated mice as well as organs of treated mice were embedded in Tissue-Tek medium and cryocut into slices of 20 µm thickness with a cryotom (Microm HM 550, Thermo Fischer). The slices were placed on glass object dishes and air dried. A slice of 5 µm was stained with haematoxylin eosin (HE) for the histological evaluation.

General setup for LA. Laser ablation was performed with a solid state laser (Nd:YAG) at a wavelength of 213 nm (NWR 213, ESI, Fremont, CA, USA), equipped with a 2 volume ablation cell. Enhancing the performance for bioimaging applications, the laser was detuned yielding a reduced maximum energy of 2 mJ in the ablation chamber, thus enabling improved fine-tuning of the applied

energy. Furthermore, the laser beam path was equipped with a square-shaped laser spot table ensuring a constant delivery of energy onto the moving sample throughout the entire diameter of the laser beam. An optical sample map of the region of interest was generated and the ablation pattern (parallel line scans) was defined. Ablation was performed at a spot size of 70 µm and a scan speed of 40 µm/s. The ablated material was transferred to the ICP-MS with He at a flow rate of 400 ml/min. Further parameters for the laser ablation process are summarized in Table 2 and for LA-ICP-MS in Table 1.

Table 2: Instrumental parameters used in laser ablation experiments

Sample Energy [mJ]	0.08-0.10
Fluence [J/cm²]	2.1-2.5
Repetition rate [Hz]	10
Laser beam shape	Square
Spot size [µm]	70
Scan speed [µm/s]	40
Transfer gas and flow rate [ml/min]	He, 400
Length per line (Standards) [mm]	2
Spacing between lines [µm]	10
Warm up [s]	10
Wash out delay [s]	15

Method development and validation. The matrix-matched standards from pig liver and the control samples were ablated in line-scans of 2 mm in length in the following order: standards (0, 1, 5, 10, 50 µg/g, two lines per concentration level), control samples (5 lines each), standards (two lines per concentration level), control samples (5 lines each), standards (two lines per concentration level). The laser and ICP-MS parameters are summarized in Table 1 and Table 2, respectively. The average gas blank was calculated for each isotope and subtracted from each individually registered data point. Additionally, the $^{102}Ru/^{115}In$, $^{195}Pt/^{185}Re$, $^{102}Ru/^{13}C$ and $^{195}Pt/^{13}C$ ratio for each data point and averages over all data points (90-110) within a line scan were calculated. The resulting average counts (or ratios) per line-scan were averaged over the six line-scans per concentration level and plotted against the concentration obtained by MW/ICP-MS yielding the respective calibration curves. The raw data of the ten lines per control sample were processed in the same manner, and their average counts (or ratios) as well as their precision were converted into concentrations and

corresponding standard deviations using the calibration curve from the LA–ICP-MS experiment. Concentrations of the homogenized control samples, obtained independently by LA–ICP-MS and by MW/ICP-MS were compared to verify accuracy and precision.

Quantitative bioimaging of mice organs. Each standard was analyzed in triplicate line scans (length: 1.5–3 mm) at least before and after scanning of a tissue section. In case the analysis time exceeded 2 h, standards were additionally measured within the ablation experiment. Length and width of the ablated area were measured for scaling purpose. The recorded files were imported into Iolite (Version 2.15)[48] as an add-on to Igor Pro (Wavemetrics, Igor Pro 6.22A). The maps of the metal distribution (^{195}Pt and ^{102}Ru) were generated with the data reduction scheme Trace_Elements following the procedures described in the manual (Iolite User Manual, Version 2.0)[49] including background subtraction and no smoothing of the visualization. The aspect ratio of the image was set according to the length and width of the ablated area to obtain accurately shaped pictures. The visualized metal distribution was scaled proportionally and superimposed on the histologic image.

Assignment of concentrations to the resulting color-coded Ru or Pt maps was performed and validated in the following manner: The instrumental drift was monitored by the standards that were run before and after the ablation experiment. In case the drift of the counts exceeded 15%, no quantitative calculations were performed; otherwise the concentration of each standard was assigned in the scale bar of the image to the corresponding average counts. In order to validate the spatially-resolved, quantitative biodistribution, the average concentration determined by MW/ICP-MS was assigned in the scale-bar as well. The quantitative image was considered to be valid, if the concentration determined by MW/ICP-MS was within the concentration pattern determined by bioimaging.

RESULTS AND DISCUSSION

A method for obtaining quantitative information on the metal distribution in organs of cisplatin- and KP1339- treated mice was developed and validated. Metal concentrations in organs originating from a single mouse were determined independently by two methodologies: LA–ICP-MS and MW followed by quantification with ICP-MS.

Method development and validation

Pig liver is well suited for the preparation of matrix-matched standards due to the absence of fascia and connective tissue as well as its availability. Details on the concentration of the standards,

determined by MW/ICP-MS, and typical calibration curves for LA–ICP-MS, obtained by ablating cryocuts of the matrix-matched standards, are available in the Supporting Information (Table S2 and Figure S1, respectively).

In order to validate the calibration for LA–ICP-MS, a tissue slice of known concentration originating from homogenized liver of a treated mouse was prepared. Homogenization is required to ensure a uniform distribution of the spiked internal standards (In, Re), to identify the best suited internal standard. This process circumvents any impact of inhomogeneous drug distribution in liver originating from animal experiments. The concentrations of the control samples (approx. 20–40 mg) were determined in triplicates by means of MW/ICP-MS as 0.257±0.039 µg/g and 22.0±1.2 µg/g for Pt and Ru, respectively. These values were considered as target values for the quantification of these elements in tissue sections of the same samples by LA–ICP-MS. The results for two slices of the homogenized mouse liver (homogenate 1 and homogenate 2) are depicted in Figure 2. Quantification only via raw counts results in recoveries for both elements in the range of 93-120% (Table S3). Internal standards, spiked to the homogenate (^{115}In, ^{185}Re) did not improve the recovery, while an internal standard being present intrinsically in the sample (^{13}C), yields improved data in the case of Ru. For Pt, recovery was worse when In was used as the internal standard, which may be due to their different masses and first ionization energies (9.0 *vs.* 5.8 eV, respectively). Although being much lighter than Pt, even ^{13}C (11.3 eV), performed better as internal standard than In, maybe due to their similar first ionization potential. Additionally, analysis of homogenates originating from the same tissue type and use of an internal standard intrinsically present, such as ^{13}C, were considered as best prerequisites to ensure uniform distribution within the sample as well as identical concentration of the internal standard between different samples. Using this approach, biased results due to inconstant internal standard concentrations were ruled out.

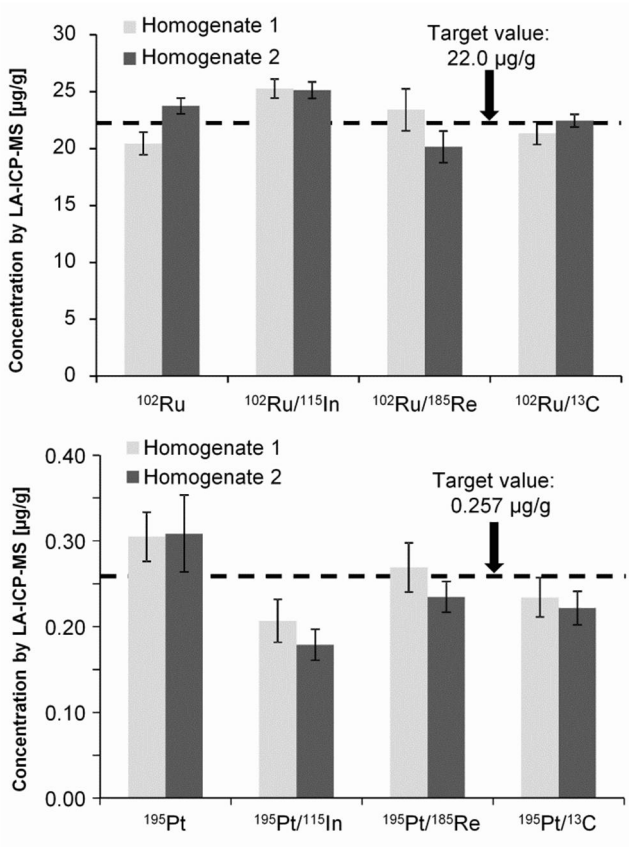

Figure 2: LA–ICP-MS-based quantification of ruthenium (top) and platinum (bottom) in homogenized liver originating from mice treated with either KP1339 or cisplatin, respectively. The dashed lines indicate the target value, obtained by quantification via MW/ICP-MS of liver samples. LA-ICP-MS based quantifications via raw counts of the metal as well as the use of internal standards ^{115}In, ^{185}Re and ^{13}C were compared with respect to their accuracy and precision (standard deviation calculated from 10 line scans of 1950 µm length each).

Ten line-scans per homogenate were conducted and the precision (expressed as relative standard deviation) ranged from 3 to 8% in case of Ru and 8 to 15% in case of Pt (Table S3), whereas none of the internal standards improved precision significantly. The higher uncertainty for Pt might be explained by its 100-fold lower concentration in liver tissue compared to the Ru sample.

However, accuracy and precision based on averages (ten line-scans, each approx. 90 data points) are not valid for bioimaging experiments. Laser ablation imaging experiments are usually optimized via scan speed of the laser, laser diameter and registration time per datapoint[20,50] but do not allow for collection of a large number of data points to obtain an average. Hence, we randomly selected one line-scan of the ruthenium and one of the platinum homogenate (Figure 3 and Figure S2). Concentrations scatter symmetrically along the scans, indicating well-homogenized samples and the absence of a concentration gradient. In case of the higher concentrated ruthenium sample, single spikes ranged from 10 up to 40 µg/g and precision over the entire line was approx. 20% giving a more realistic picture on the interpretation of bioimaging data. Analysis of the Pt sample (< 0.5 µg/g) showed that spatially-resolved quantitative data is not meaningful in the experimental setting:

although the average over ten line-scans was still satisfying with regard to precision and accuracy (Table S3), precision within a single line-scan was lower than 30% and spikes ranged from 0.05 to 0.8 µg/g (target concentration: 0.257 µg/g), which equals recoveries from 19 to 311%. Hence, intensities of peaks being distinctly different from neighbouring ones in bioimaging experiments should be interpreted with caution, especially in low concentrated samples (sub µg/g range).

Data analysis employing internal standards (^{13}C, ^{115}In, ^{185}Re) demonstrated that neither of them improved the precision significantly (Figure S2), thus, supporting that quantification solely via raw counts and matrix-matched standards is feasible[36,39,42,51]. Hence, we decided to perform quantitative LA experiments without internal standard, but ensured that instrumental drift during the ablation experiments was monitored by running calibration standards at least three times (at the beginning, during the ablation experiment and at the end of the sample run) and evaluated their precision. In case precision exceeded 15%, raw counts are reported instead of quantitative data.

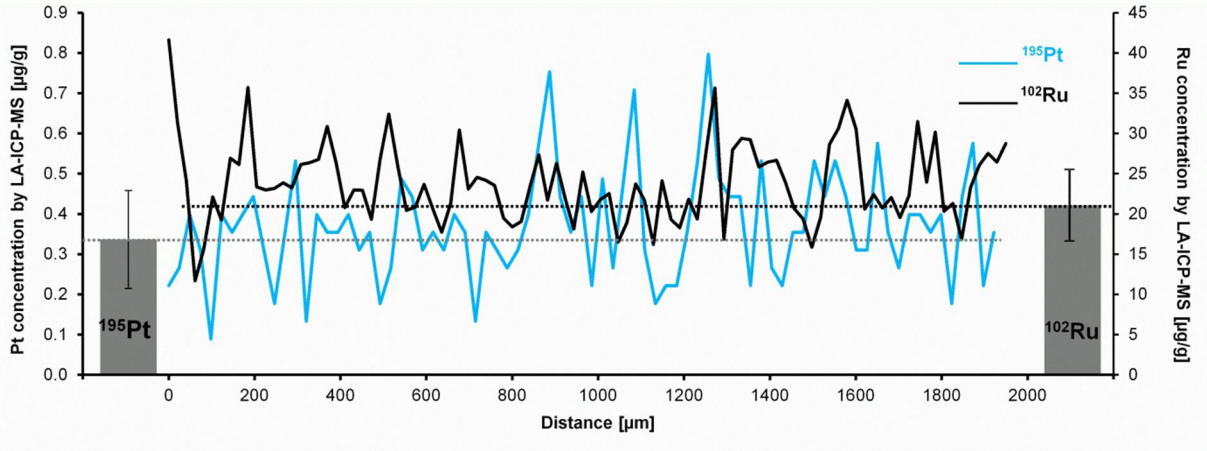

Figure 3: Concentrations of Ru and Pt along a single line-scan (1950 µm) as determined by LA–ICP-MS in homogenized mouse liver originating from mice treated with either KP1339 or cisplatin, respectively. The bar charts represent the average and standard deviation of the line-scan. The target concentrations are 22.0 µg/g for Ru and 0.257 µg/g for Pt. The impact of internal standardization (^{13}C, ^{115}In, ^{185}Re) is visualized in Figure S2 in the same manner.

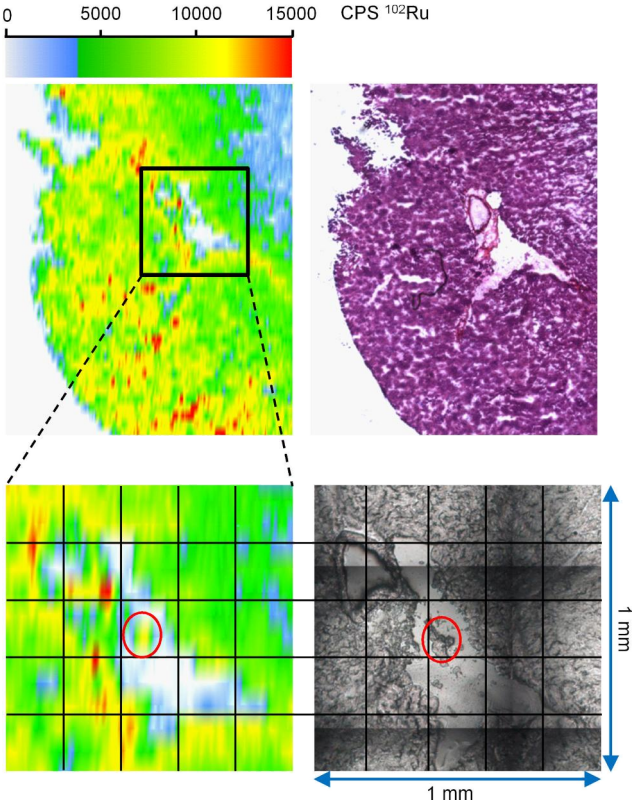

Figure 4: Pictures of the LA-scan (left) and a consecutive HE stained slice (right top) of kidney originating from a KP1339-treated mouse. The applied parameters for LA (70 µm laser diameter, 40 µm/s scan speed) allowed identification of a small piece of tissue (100 µm, red circles) within a tissue free area (greyscale picture prior to ablation).

In order to estimate the spatial resolution of the experimental setting, ablation was performed in parallel, horizontal line-scans. Hence, the diameter of the laser limits the vertical resolution to 70 µm with the laser parameters used. The horizontal resolution (along the line) was mainly impacted by the scan speed and dwell time (40 µm/s and 0.1 s). Thus, the theoretical limit equals a pixel size of 70 × 4 µm. A detailed picture of a KP1339-treated kidney (Figure 4) features a tissue structure of approximately 100 × 100 µm in size (red circle). This structure is clearly visible in the corresponding laser ablation image, indicating that meaningful imaging data is obtained for structures exceeding 100 µm in size (Figure 4).

Bioimaging of cisplatin- and KP1339-treated viscera

Viscera of mice treated either with KP1339 or cisplatin were obtained and the respective distribution of the metal, expressed as counts per second (CPS), was determined within kidney and spleen (Figure 5) as well as muscle and liver (Figure S3, Supporting Information). In order to validate the concentrations determined with LA–ICP-MS, 20–40 mg of tissue was digested in a microwave using half-concentrated nitric acid and analyzed by ICP-MS. The resulting average metal concentrations for each organ are summarized in Table 3. Despite the ablation was performed on different days, the

rank order of average CPS in bioimages followed the concentrations determined by MW/ICP-MS: Ru concentrations from MW/ICP-MS experiments decreased in the order liver ≥ kidney >> spleen > muscle and average CPS recorded by LA were estimated as 12000 for liver and kidney, 7000 for spleen, and 3000 for muscle. Additionally, the MW/ICP-MS procedure was used as an independent methodology to assess the accuracy of the quantitative Pt distribution in kidney and Ru distribution in liver and kidney in the following manner: the average Ru concentration determined by MW/ICP-MS (e.g. 22.6 ± 0.8 µg/g in liver, Table 3) was indicated with an asterisk in the color bar (Figure 5 and Figure S3, Supporting Information), which shows that the concentration from MW/ICP-MS is in accordance with the concentrations determined by LA–ICP-MS. In case of the kidneys, the Ru and Pt concentrations determined by MW/ICP-MS corresponded to concentrations found in the cortex, hence again proving validity of the approach. When determining the quantitative distribution of Pt in a liver originating from a cisplatin-treated mouse the instrumental drift exceeded 15% and the quantitative data was therefore considered not valid.

Table 3: Metal concentrations in organs of mice treated either with cisplatin or KP1339. Concentrations were determined after MW digestion of samples by ICP-MS. The data correspond to the same mice that were cryocut and ablated as depicted previously. The results are given as mean ± standard deviation in case of cisplatin and as mean ± span in case of KP1339. Concentrations of Pt in muscle and spleen were not determined (n.d.) due to insufficient sample material.

	Concentration [µg/g]	
Organ	**Cisplatin** (Pt, n=3)	**KP1339** (Ru, n=2)
Liver	3.9 ± 1.2	22.6 ± 0.8
Kidney	11.2 ± 0.6	20.5 ± 2.2
Muscle	n.d.	2.9 ± 0.3
Spleen	n.d.	6.5 ± 0.4

Both metals were found to be homogenously distributed in the liver tissue, whereas the metal distribution in kidney tissue correlated with the functional differentiation of the organ. The Pt concentration in the cortex was found to be about 10-times higher than in the medulla (9 and < 0.8 µg/g, respectively). Note that the reported absolute values do not consider biological variations as they are based on experiments with a single mouse per metal compound. However, our data obtained for cisplatin-treated mice is in good agreement with most data reported previously, using also LA–ICP-MS,[42-44] although treatment regimens as well as preparation of samples and standards varied significantly (see Table S4, Supporting Information). So far, only two of them dealt with spatially-resolved, quantitative bioimaging:[42,44] Zoriy *et al.* studied Pt distribution in frozen sections of kidney originating from cisplatin treated mice (3 mg/kg for 60 min) first and reported highest

concentrations in the medulla and progressively decreasing amounts to the periphery.[42] In contrast, Reifschneider *et al.* not only investigated murine kidney and cochlea tissue affected by cisplatin treatment but also the testes as therapeutic target tissue and reported Pt biodistribution quantitatively. Samples were obtained from mice treated with cisplatin (15 mg/kg) for 1 h or 4 days and embedded in a cold polymerizing resin, which was used for preparation of standards as well. The highest concentrations of 85 and 2 µg/g were detected in the cortico-medullary region upon treatment for 1 h and 4 days, respectively, and no significant Pt accumulation was detected in the medulla.[44] These findings are in good agreement with our data (approx. 9 µg/g in the cortex), considering the treatment time of 24 h in our case. Moreno-Gordaliza *et al.* investigated formalin-fixed paraffin-embedded (FFPE) kidneys.[43] In this study, Pt was found to be enriched by a factor of 10 in cortex in comparison with the medulla, which is also in accordance with our results. On the other hand, quantitative Pt concentrations differ substantially despite comparable dosages (16 mg/kg for 3 days *vs.* 15 mg/kg for 1 day in our study) and identical route of applications (i.p.). While quantification is based on LA–ICP-MS in both cases, the sample and standard preparation varied considerably (e.g. FFPE tissue) yielding loss of quantitative spatial resolution and some experimental details remain ambigous. Our approach (treatment 15 mg/kg, 1 day) based on the LA–ICP-MS analysis of cryocuts and matrix-matched standards for calibration was chosen to obtain spatially-resolved quantitative information. The reported concentrations of < 0.8 µg/g in the medulla and approximately 9 µg/g in the cortex, as estimated from Figure 5, correspond to wet tissue. Furthermore, this was independently confirmed by determining the Pt content of the same kidney used for preparation of cryocuts by MW/ICP-MS, which yielded an average Pt concentration of 11.2 ± 0.6 µg/g (Table 3), thereby proving the accuracy of our quantitative laser ablation procedure.

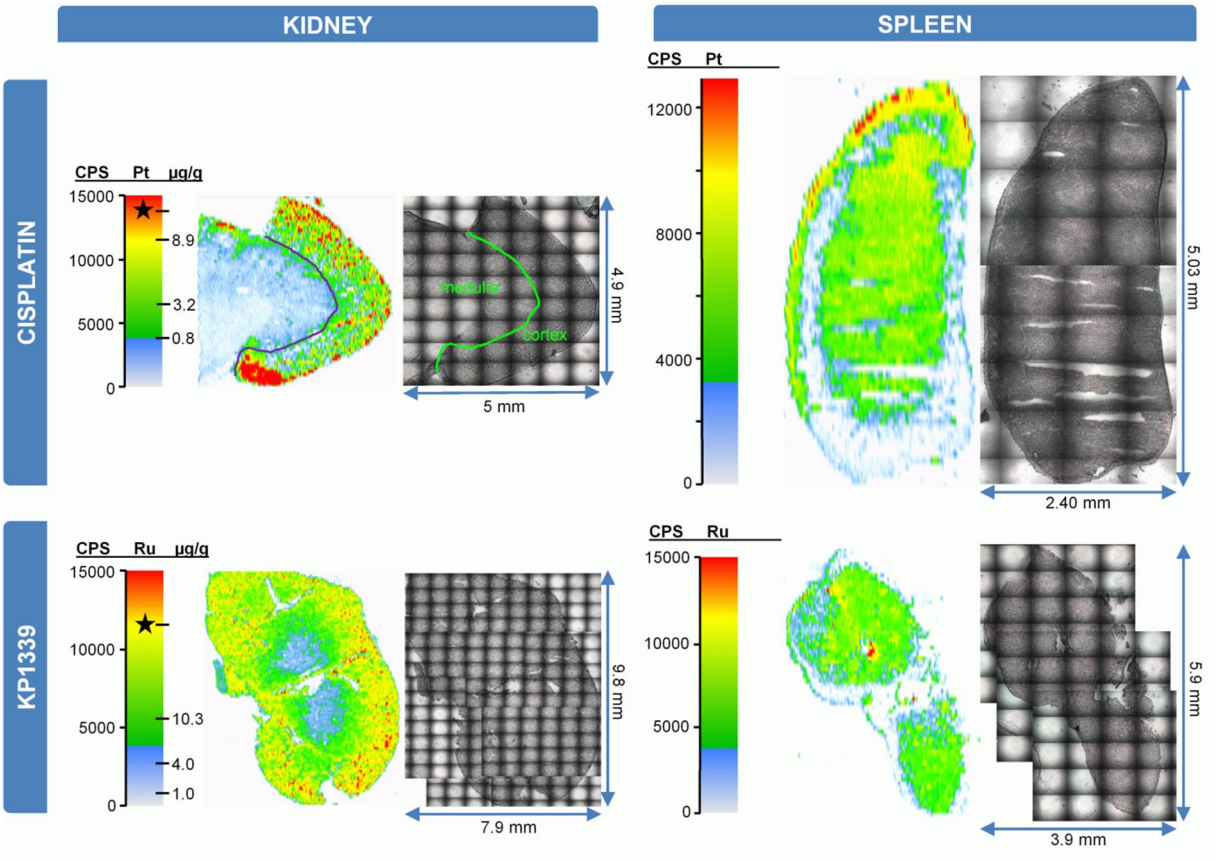

Figure 5: Distribution of ^{195}Pt and ^{102}Ru in kidney and spleen of mice treated either with cisplatin or KP1339. Visualization was based on 128 and 76 parallel line scans (scan direction left to right, alignment of the lines from top to bottom) for Ru-containing viscera and 63 and 64 for Pt. The corresponding greyscale images were recorded with the built-in camera of the laser ablation system prior to ablation of the sample. The color scales represent the recorded counts per second (CPS) of the registered metal ion isotopes by LA–ICP-MS. Quantitative amounts of Pt and Ru in kidney were obtained by ablating matrix matched standards within the same run. In these cases, concentrations obtained by MW/ICP-MS were appropriately assigned to the color scale bar with an asterisk. Their corresponding colors according to the scale are in good accordance with the colors available in pictures obtained by LA–ICP-MS, proving validity of the method in real samples. Analysis of spleen was performed without simultaneous ablation of standards.

The observed accumulation of Pt in cortex of the kidney is in accordance with its toxicity for proximal tubule cells, located in the cortico-medullary junction.[52] However, drawing conclusions on potential side effects solely on the basis of accumulation is not justified: Ru originating from KP1339 possesses a comparable distribution pattern in kidneys, but in contrast to cisplatin no severe side effects (such as nephrotoxicity) have been observed in preclinical or clinical trials.[10,11] Additionally, we compared stained kidney sections from cisplatin and KP1339-treated mice histologically and no pathologic alterations indicating acute tubular damage were observed (Supporting Information, Figures S4 and S5). Studies focusing on cisplatin nephrotoxicity report visible histologic damage in renal tissue after cisplatin treatment of rats (5 mg/kg for 5 days[52] or 16 mg/kg for 3 days).[43] As degenerative changes in proximal tubule tissue become visible after 3-5 days at earliest,[53] the short treatment-time with cisplatin in our experiment (24 h) explains the discrepancy at histologic level.

Pt and Ru are homogenously distributed in muscle tissue (Supporting information, Figure S3) and distribution in spleen exhibited regions with enriched amounts of metals for both compounds (Figure 5, left).

CONCLUSION

Quantification of elemental distributions in biological samples studied by LA–ICP-MS suffers from a lack of certified reference materials for the analyte of interest and currently no standardized approach for the application of internal standards is available. Therefore we focused in this paper on the method development and validation of a quantitative LA–ICP-MS bioimaging experiment in organs of mice treated with the anticancer agents KP1339 or cisplatin. Analysis of liver homogenates by a single line-scan resulted in a realistic estimation of the precision for tissue imaging with a relative standard deviation of approximately 20%, while averaging over line-scans only pretended high accuracy (70-120%) and precision (3-15%). Applying internal standards such as ^{115}In, ^{185}Re and ^{13}C did not improve the quality of the data and was not mandatory given instrumental response is stable over time with a drift of less than 15% during the entire ablation experiment. The experimental resolution of the elemental distributions was determined to be approximately 100 µm *via* corresponding histological structures in optical images of the ablated area.

Using this method, the spatially-resolved biodistribution of KP1339 in a series of organs was studied for the first time, exhibiting distribution patterns similar to cisplatin. Because of the low number of test animals used, the absolute values on organ distributions have to be taken carefully. Both compounds were enriched in the cortex of the kidney in comparison with the medulla, a homogenous distribution was determined in the liver as well as in muscle tissue and areas of the spleen showed also higher metal concentrations. The viscera were additionally digested in a microwave and the concentrations as determined by direct infusion ICP-MS confirmed those determined by LA–ICP-MS imaging. Therefore the validity of the data in real world samples was demonstrated in an independent experiment. Moreover, our data reveal that no toxic alterations at histologic level are observed after treatment of mice with KP1339, although the ruthenium concentration in tissue was much higher than the platinum concentration. This is in good agreement with the outstanding lack of severe side effects of KP1339 treatment.[11]

ACKNOWLEDGMENTS

C. G. H. is grateful for the financial support provided by the Austrian Science Fund (Project Number I496-B11; postdoctoral fellowship to A.E.E.), the University of Auckland, Genesis Oncology Trust, and the Royal Society of New Zealand. We would like to thank the members of the COST actions D39 and

CM1105 for useful discussions. The authors are indebted to Dr. Michael Reithofer and Dr. Werner Ginzinger for preparation of cisplatin and KP1339, respectively. Lucas Prieto Gonzáles-Posada is acknowledged for assisting in sample preparation, Gerlinde Grabmann for fruitful discussion and Ute Jungwirth for providing the picture of the mouse in Scheme S1.

REFERENCES

1. J. Reedijk, *Chem. Rev.*, 1999, **99**, 2499-2510.
2. N. P. E. Barry and P. J. Sadler, *Chem. Commun.*, 2013, **49**, 5106-5131.
3. M. A. Jakupec, M. Galanski and B. K. Keppler, *Rev. Physiol. Biochem. Pharmacol.*, 2003, **146**, 1-53.
4. X. Yao, K. Panichpisal, N. Kurtzman and N. Kenneth, *Am. J. Med. Science*, 2007, **334**, 115-124.
5. D. Lebwohl and R. Canetta, *Eur. J. Cancer*, 1998, **34**, 1522-1534.
6. M. A. Jakupec, M. Galanski, V. B. Arion, C. G. Hartinger and B. K. Keppler, *Dalton Trans.*, 2008, 183-194.
7. C. G. Hartinger, S. Zorbas-Seifried, M. A. Jakupec, B. Kynast, H. Zorbas and B. K. Keppler, *J. Inorg. Biochem.*, 2006, **100**, 891-904.
8. C. G. Hartinger, M. A. Jakupec, S. Zorbas-Seifried, M. Groessl, A. Egger, W. Berger, H. Zorbas, P. J. Dyson and B. K. Keppler, *Chem. Biodiversity*, 2008, **5**, 2140-2155.
9. A. Bergamo, C. Gaiddon, J. H. M. Schellens, J. H. Beijnen and G. Sava, *J. Inorg. Biochem.*, 2012, **106**, 90-99.
10. D. S. Thompson, G. J. Weiss, S. F. Jones, H. A. Burris, R. K. Ramanathan, J. R. Infante, J. C. Bendell, A. Ogden and D. D. Von Hoff, *J. Clin. Oncol.*, 2012 (suppl), **30**, abstr 3033.
11. R. Trondl, P. Heffeter, C. R. Kowol, M. A. Jakupec, W. Berger and B. K. Keppler, *Chem. Sci.*, 2014, **in press**.
12. J. Arrowsmith, *Nat. Rev. Drug Discovery*, 2011, **10**, 1-1.
13. J. Arrowsmith and P. Miller, *Nat. Rev. Drug Discovery*, 2013, **12**, 569.
14. C. S. Allardyce, P. J. Dyson, F. R. Abou-Shakra, H. Birtwistle and J. Coffey, *Chem. Commun.*, 2001, 2708-2709.
15. I. Khalaila, A. Bergamo, F. Bussy, G. Sava and P. J. Dyson, *Int. J. Oncol.*, 2006, **29**, 261-268.
16. J. S. Becker and N. Jakubowski, *Chem. Soc. Rev.*, 2009, **38**, 1969-1983.
17. J. S. Becker, M. Zoriy, A. Matusch, B. Wu, D. Salber, C. Palm and J. S. Becker, *Mass Spectrom. Rev.*, 2010, **29**, 156-175.
18. I. Konz, B. Fernández, M. Fernández, R. Pereiro and A. Sanz-Medel, *Anal. Bioanal. Chem.*, 2012, **403**, 2113-2125.
19. J. S. Becker, M. V. Zoriy, C. Pickhardt, N. Palomero-Gallagher and K. Zilles, *Anal. Chem.*, 2005, **77**, 3208-3216.
20. C. Giesen, T. Mairinger, L. Khoury, L. Waentig, N. Jakubowski and U. Panne, *Anal. Chem.*, 2011, **83**, 8177-8183.
21. D. Hare, C. Austin and P. Doble, *Analyst*, 2012, **137**, 1527-1537.

22. D. Pozebon, V. L. Dressler, M. F. Mesko, A. Matusch and J. S. Becker, *J. Anal. At. Spectrom.*, 2010, **25**, 1739-1744.
23. C. Austin, D. Hare, T. Rawling, A. M. McDonagh and P. Doble, *J. Anal. At. Spectrom.*, 2010, **25**, 722-725.
24. H. Sela, Z. Karpas, H. Cohen, Y. Zakon and Y. Zeiri, *Int. J. Mass Spectrom.*, 2011, **307**, 142-148.
25. J. A. T. Pugh, A. G. Cox, C. W. McLeod, J. Bunch, B. Whitby, B. Gordon, T. Kalber and E. White, *J. Anal. At. Spectrom.*, 2011, **26**, 1667-1673.
26. K. Jurowski, S. Walas and W. Piekoszewski, *Talanta*, 2013, **115**, 195-199.
27. C. Austin, F. Fryer, J. Lear, D. Bishop, D. Hare, T. Rawling, L. Kirkup, A. McDonagh and P. Doble, *J. Anal. At. Spectrom.*, 2011, **26**, 1494-1501.
28. D. A. Frick and D. Gunther, *J. Anal. At. Spectrom.*, 2012, **27**, 1294-1303.
29. C. Giesen, L. Waentig, T. Mairinger, D. Drescher, J. Kneipp, P. H. Roos, U. Panne and N. Jakubowski, *J. Anal. At. Spectrom.*, 2011, **26**, 2160-2165.
30. L. Waentig, N. Jakubowski, H. Hayen and P. H. Roos, *J. Anal. At. Spectrom.*, 2011, **26**, 1610-1618.
31. I. Konz, B. Fernández, M. L. Fernández, R. Pereiro, H. González, L. Álvarez, M. Coca-Prados and A. Sanz-Medel, *Anal. Bioanal. Chem.*, 2013, **405**, 3091-3096.
32. D. Drescher, C. Giesen, H. Traub, U. Panne, J. Kneipp and N. Jakubowski, *Anal. Chem.*, 2012.
33. H. A. O. Wang, D. Grolimund, C. Giesen, C. N. Borca, J. R. H. Shaw-Stewart, B. Bodenmiller and D. Günther, *Anal. Chem.*, 2013, **85**, 10107-10116.
34. A. J. Managh, S. L. Edwards, A. Bushell, K. J. Wood, E. K. Geissler, J. A. Hutchinson, R. W. Hutchinson, H. J. Reid and B. L. Sharp, *Anal. Chem.*, 2013.
35. B. Jackson, S. Harper, L. Smith and J. Flinn, *Anal. Bioanal. Chem.*, 2006, **384**, 951-957.
36. A. Matusch, C. Depboylu, C. Palm, B. Wu, G. U. Höglinger, M. K. H. Schäfer and J. S. Becker, *J. Am. Soc. Mass Spectrom.*, 2010, **21**, 161-171.
37. J. S. Becker, *Int. J. Mass Spectrom.*, 2010, **289**, 65-75.
38. D. J. Hare, J. K. Lee, A. D. Beavis, A. van Gramberg, J. George, P. A. Adlard, D. I. Finkelstein and P. A. Doble, *Anal. Chem.*, 2012, **84**, 3990-3997.
39. M. V. Zoriy, M. Dehnhardt, G. Reifenberger, K. Zilles and J. S. Becker, *Int. J. Mass Spectrom.*, 2006, **257**, 27-33.
40. M. V. Zoriy, M. Dehnhardt, A. Matusch and J. S. Becker, *Spectrochim. Acta, Part B*, 2008, **63**, 375-382.
41. D. Hare, F. Burger, C. Austin, F. Fryer, R. Grimm, B. Reedy, R. A. Scolyer, J. F. Thompson and P. Doble, *Analyst*, 2009, **134**, 450-453.
42. M. Zoriy, A. Matusch, T. Spruss and J. S. Becker, *Int. J. Mass Spectrom.*, 2007, **260**, 102-106.
43. E. Moreno-Gordaliza, C. Giesen, A. Lázaro, D. Esteban-Fernández, B. Humanes, B. Cañas, U. Panne, A. Tejedor, N. Jakubowski and M. M. Gómez-Gómez, *Anal. Chem.*, 2011, **83**, 7933-7940.
44. O. Reifschneider, C. A. Wehe, K. Diebold, C. Becker, M. Sperling and U. Karst, *J. Anal. At. Spectrom.*, 2013, **28**, 989-993.
45. D. Gholap, J. Verhulst, W. Ceelen and F. Vanhaecke, *Anal. Bioanal. Chem.*, 2012, **402**, 2121-2129.
46. S. C. Dhara, *Indian J. Chem.*, 1970, **8**, 193-194.
47. B. K. Keppler, *Nikii Pharma Inc., USA*, 2008.

48. C. Paton, J. Hellstrom, B. Paul, J. Woodhead and J. Hergt, *J. Anal. At. Spectrom.*, 2011, **26**, 2508-2518.
49. http://www.iolite.org.au/Iolite.html.
50. J. Lear, D. Hare, P. Adlard, D. Finkelstein and P. Doble, *J. Anal. At. Spectrom.*, 2012, **27**, 159-164.
51. J. S. Becker, U. Breuer, H.-F. Hsieh, T. Osterholt, U. Kumtabtim, B. Wu, A. Matusch, J. A. Caruso and Z. Qin, *Anal. Chem.*, 2010, **82**, 9528-9533.
52. D. Sheikh-Hamad, W. Cacini, A. Buckley, J. Isaac, L. Truong, C. Tsao and B. Kishore, *Arch. Toxicol.*, 2004, **78**, 147-155.
53. J. P. Fillastre and G. Raguenez-Viotte, *Toxicol. Lett.*, 1989, **46**, 163-175.